UCH-L1 physically interacts with tubulin

To understand the molecular mechanism underlying toxic gain of function by UCH-L1, we attempted to identify UCH-L1^{I93M}-interacting proteins by coIP assay and subsequent LC-MS/MS analysis (Fig. 5A). A database search of the peptide sequences obtained identified α-tubulin as a UCH-L1^{I93M}-interacting protein (Supplementary Material, Table S1). The interaction between UCH-L1 and endogenous α-tubulin was confirmed with transiently expressed UCH-L1 (Fig. 5B and C). The interaction of UCH-L1^{I93M} with α-tubulin was increased compared with that of UCH-L1^{WT} (Fig. 5B). We detected the interaction of endogenous α-tubulin with endogenous UCH-L1 using Neuro2a cells (Fig. 5D). Tubulin is composed of a heterodimer of α- and β-tubulin, and we confirmed, using native-PAGE, that tubulin exists as a heterodimer in cell lysates in coIP experimental conditions (data not shown), indicating that UCH-L1 interacts with tubulin. Indeed, β-tubulin was also precipitated with UCH-L1 (Supplementary Material, Fig. S3). In contrast to tubulin, interaction of β-actin with UCH-L1 was not detected (Fig. 5C). To test whether UCH-L1 directly interacts with tubulin, we performed pull-down assay using recombinant UCH-L1 and purified tubulin. Direct interaction of UCH-L1 with tubulin was observed (Fig. 5E).

Since the interactions between UCH-L1 and proteins over 30 kDa are increased by carbonyl modification or I93M mutation of UCH-L1, we tested the effects of HAE on the interaction of UCH-L1 with tubulin. We found that HAE modification of UCH-L1 promotes interactions between UCH-L1 and tubulin (Fig. 5F, G and I). In addition, a coIP assay using C90S, C132S and C152S UCH-L1 mutants showed less binding of UCH-L1^{C90S} to tubulin than UCH-L1^{WT} did, when cells were treated with HNE or HHE (Fig. 5G–I), indicating that the increased interaction of UCH-L1 with tubulin is caused by the HAE modification of Cys-90 of UCH-L1. These results are consistent with the results showing that the HAE modification of Cys-90 of UCH-L1 promotes the interaction of UCH-L1 with multiple proteins. The I93M mutation and HNE modification of UCH-L1 also promote direct interactions between UCH-L1 and tubulin (data not shown). Thus, UCH-L1^{I93M} and HNE-UCH-L1 also exhibit common biochemical properties with respect to the interactions with tubulin.

Both UCH-L1^{I93M} and carbonyl-modified UCH-L1 aberrantly promote tubulin polymerization

Microtubules are dynamic polymers composed of tubulin that continuously grow and shorten through tubulin addition and loss at the microtubule ends. Microtubule-stabilizing agents such as paclitaxel, which promote tubulin polymerization and suppress microtubule dynamics, are effective chemotherapeutic agents for the treatment of many cancers. However, neuropathy is a major adverse effect of microtubule-stabilizing agents-based chemotherapy (35). Paclitaxel induces apoptosis in cortical neurons by a mechanism independent of its cell cycle effects, because postnatal cortical neurons are postmitotic (36). These findings indicate that tubulin polymerization must be tightly regulated for neurons to function and remain viable. Furthermore, abnormal microtubule dynamics and tubulin polymerization are associated with several neurodegenerative diseases including frontotemporal dementia and parkinsonism linked to chromosome 17 (37,38). Therefore, we examined the effects of UCH-L1^{WT}, UCH-L1^{I93M} and HNE-UCH-L1 on tubulin polymerization using an *in vitro* assay. Interestingly, both UCH-L1^{I93M} and HNE-UCH-L1 promote tubulin polymerization, although UCH-L1^{WT} had almost no effect on it (Fig. 6A and B). Promotion of tubulin polymerization may result in a stabilization of microtubules because of the dynamic instability of microtubules. To test whether abnormal UCH-L1 also promotes tubulin polymerization in mammalian cells, we analyzed the amounts of soluble, polymeric and total tubulin in cells expressing UCH-L1^{I93M}. Although transient expression of UCH-L1^{I93M} had no effect on the amount of total tubulin (Fig. 5B), cells stably expressing UCH-L1^{I93M} contained increased amount of total tubulin compared with control cells or cells expressing other UCH-L1 variants (Fig. 6C). Consistent with the *in vitro* polymerization assay, the amount of polymeric tubulin was increased in cells expressing UCH-L1^{I93M}, whereas the amount of soluble tubulin was not (~1.4 and 1.0-fold increase, respectively, compared with the amount of tubulin in cells expressing UCH-L1^{WT}) (Fig. 6D). The amount of β-actin was not affected by the expression of UCH-L1 variants (Fig. 6C and D), also consistent with the results showing that UCH-L1 does not interact with β-actin. We did not detect specific interaction of UCH-L1 with polymerized tubulin (Fig. 6E), indicating that UCH-L1 may not interact with microtubules, although the possibility is not excluded that they can interact under certain conditions or at a limited number of sites such as the microtubule ends.

Since D30K and C90S mutations had no effect on the interaction of UCH-L1 and tubulin (Fig. 5B), we speculated that the tubulin-binding region of UCH-L1 is different from ubiquitin-binding region. To elucidate the amino acid residues of UCH-L1 involved in the interaction with tubulin and to show that modulation of tubulin polymerization is caused by the increased interaction of UCH-L1 with tubulin, we made a series of alanine substitutions of basic and acidic residues located on the surface of UCH-L1 and performed coIP assays using these mutants (Fig. 7A; Supplementary Material, Fig. S3). The R63A and H185A mutants displayed increased interactions with tubulin (Fig. 7A), indicating that Arg-63 and His-185, which are distinct from the ubiquitin-binding region (Fig. 7B), are involved in this interaction. The increased interactions of R63A and H185A UCH-L1 with tubulin may be caused by altered ionic interactions. In contrast to the I93M mutant or HNE-UCH-L1, the R63A mutant caused a decrease in tubulin polymerization (Fig. 7C). Although UCH-L1^{R63A} has opposite effects to the I93M mutant or HNE-UCH-L1, it also modulated tubulin polymerization. Thus, modulation of tubulin polymerization by UCH-L1 variants is caused by the abnormally increased interaction of UCH-L1 with tubulin.

From our results, we hypothesized that UCH-L1^{I93M}-associated neurodegeneration or PD is at least partly mediated by aberrant tubulin polymerization. Therefore, we tested the effects of UCH-L1^{I93M} and paclitaxel on neuronal cell death using differentiated Neuro2a cells, which

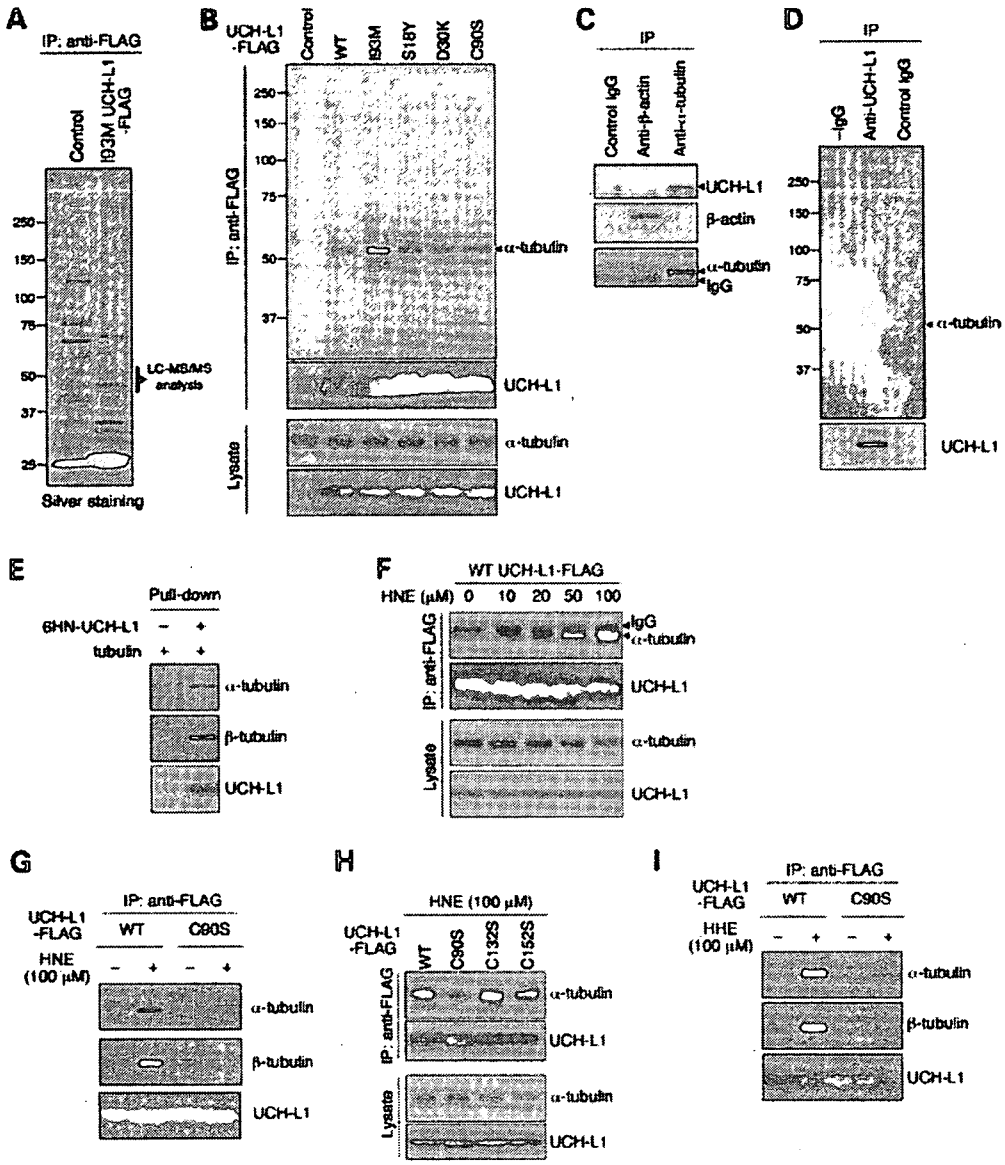

Figure 5. Physical interactions of UCH-L1 with tubulin. (**A**) Lysates of HeLa cells transfected with the indicated constructs (control: GFP) were immunoprecipitated with anti-FLAG antibody and analyzed by silver staining. Proteins ~50 kDa in size were subjected to LC-MS/MS analysis. (**B**) Lysates of COS-7 cells transfected with the indicated constructs (control: empty vector) were immunoprecipitated with anti-FLAG antibody and analyzed by immunoblotting. (**C**) Lysates of NIH-3T3 cells stably expressing FLAG-HA-tagged UCH-L1 were immunoprecipitated with the indicated antibodies and analyzed by immunoblotting. (**D**) Lysates of Neuro2a cells were immunoprecipitated with control IgG or anti-UCH-L1 antibody and analyzed by immunoblotting. –IgG, without IgG. (**E**) A pull-down assay was performed using the indicated purified proteins. [(**F**)–(**I**)] COS-7 cells transfected with the indicated constructs were treated with the indicated concentrations of HNE. Lysates were immunoprecipitated with anti-FLAG antibody and analyzed by immunoblotting.

have been used to assess the toxicity of mutant proteins linked to neurodegenerative diseases (17,39,40). We confirmed that paclitaxel does not interfere with the interaction between UCH-L1 and tubulin (data not shown). Treatment of cells with 5 μM paclitaxel slightly but significantly elevated cell death in cells expressing UCH-L1^{I93M}, but had no effect in cells expressing UCH-L1^{WT} (Fig. 6F). This indicated that the toxicity of UCH-L1^{I93M} may be at least in part mediated by aberrant microtubule dynamics or tubulin polymerization. Given that tightly regulated tubulin polymerization is necessary for neurons to be viable, our findings strongly suggest that aberrant tubulin polymerization caused by UCH-L1^{I93M} underlies the toxic gain of function of mutant UCH-L1, and that carbonyl-modified UCH-L1 also functions as a toxic protein in neurons. We propose that interactions of mutant or carbonyl-modified UCH-L1 with other proteins, including tubulin, constitute one of the causes of not only familial PD, but also sporadic PD (Fig. 7D).

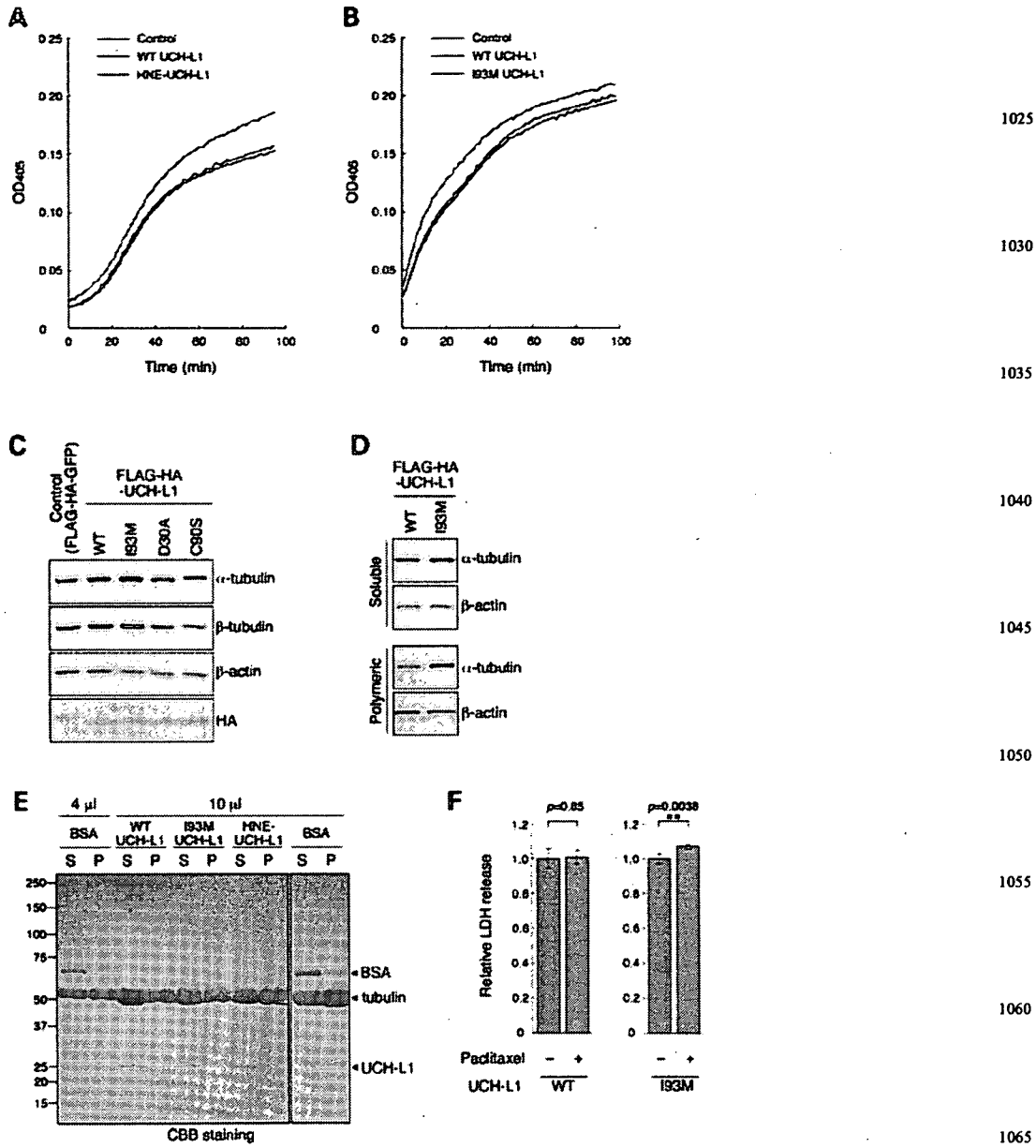

Figure 6. Effects of the I93M mutation and HNE modification of UCH-L1 on tubulin polymerization. [(**A**) and (**B**)] A tubulin polymerization assay was performed in the absence (control) or in the presence of recombinant UCH-L1. The assays were performed at least three times; representative results are shown. [(**C**) and (**D**)] Total lysates (C), soluble tubulin fractions and polymeric tubulin fractions (D) of NIH-3T3 cells stably expressing FLAG-HA-tagged UCH-L1 were analyzed by immunoblotting. (**E**) Interactions of proteins with microtubules. After the tubulin polymerization assay, the polymerized tubulin was pelleted by centrifugation. The indicated volumes of samples from the supernatants (S) and the pellets (P) were analyzed by CBB staining. BSA was used as a control that does not specifically interact with microtubules. The amount of BSA detected in the pellet fraction was approximately one-twelfth of the amount detected in the supernatant fraction. UCH-L1 levels in the pellet fraction were below detectable levels. (**F**) Differentiated Neuro2a cells transfected with the indicated constructs were incubated with or without 5 μM paclitaxel for 24 h. Cell death was assessed by a lactate dehydrogenase release assay. Data are expressed as the means ± SD ($n = 4$). $^{**}P < 0.01$ (*t*-test).

DISCUSSION

Our previous study using CD suggests that the I93M mutation increases the β-sheet content, but reduces the α-helix content of UCH-L1 (9). We have also shown, using small-angle neutron scattering, that UCH-L1^{WT} has an ellipsoidal shape, whereas UCH-L1^{I93M} has a more globular shape in an aqueous solution (10). However, the biochemical and molecular properties of UCH-L1^{I93M} in mammalian cells, as well as the molecular mechanisms that underlie UCH-L1^{I93M}-associated PD, have not been elucidated. In this study, we have shown that, compared with UCH-L1^{WT}, UCH-L1^{I93M} displays

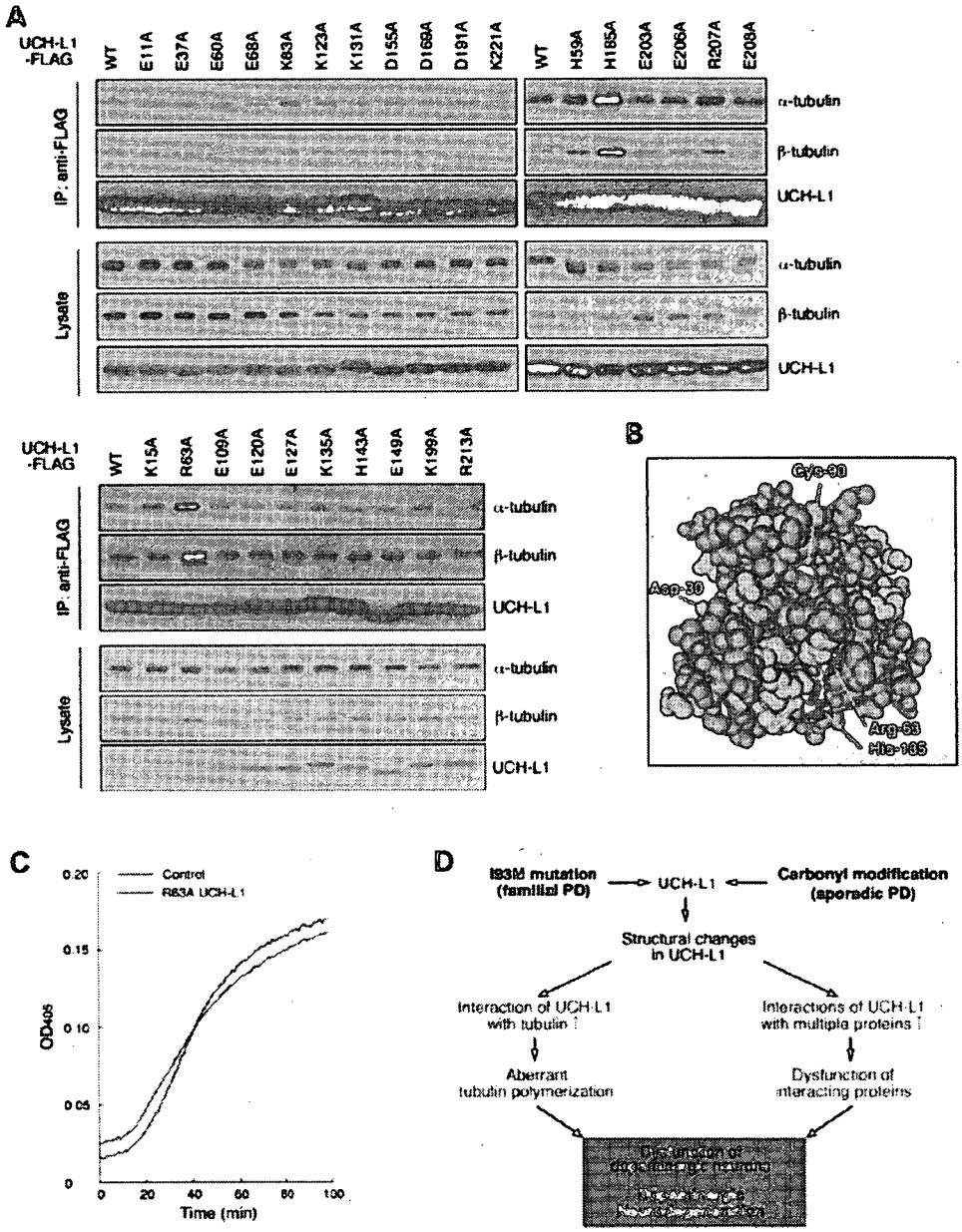

Figure 7. Amino acid residues of UCH-L1 involved in the interaction with tubulin. **(A)** Alanine-scanning mutagenesis of UCH-L1. Lysates of COS-7 cells transfected with the indicated constructs were immunoprecipitated with anti-FLAG antibody and analyzed by immunoblotting. **(B)** Structural model for human UCH-L1. Cys-90 is shown in blue, Arg-63 and His-185 are in magenta and basic and acidic amino acid residues that had no effect on tubulin interaction (Figs 5B and7A) are shown in white, using NCBI's structural model (mmdbId:38174). **(C)** A tubulin polymerization assay was performed in the absence (control) or in the presence of recombinant UCH-L1. **(D)** Schematic representation of a model for the roles of UCH-L1^{I93M} and carbonyl-modified UCH-L1 in PD. The I93M mutation (as occurs in familial PD associated with UCH-L1^{I93M}) and carbonyl modification (as occurs in sporadic PD) cause conformational changes in UCH-L1. Owing to the excess of oxidative stresses including HNE (in the case of sporadic PD) and the abundant expression of UCH-L1 in dopaminergic neurons, abnormal UCH-L1 proteins are overproduced in dopaminergic neurons. Abnormal UCH-L1 interacts with tubulin and aberrantly modulates tubulin polymerization. The aberrant interactions of UCH-L1 variants with multiple proteins may also cause dysfunctions of interacting proteins. The deregulations of abnormal UCH-L1-interacting proteins, including tubulin, result in dysfunction of dopaminergic neurons, leading to neurodegeneration.

increased insolubility, which is characteristic of several neurodegenerative disease-linked mutants, aberrantly elevated interactions with multiple proteins over 30 kDa and decreased interaction with monoubiquitin (Fig. 1). Taken together, our new and previous findings indicate that the I93M mutation in UCH-L1 alters its conformation, resulting in changes in the biochemical properties of UCH-L1.

Similar to UCH-L1^{I93M}, other dominantly inherited neurodegenerative disease-linked mutants, such as mutant SOD1 and mutant α-synuclein, cause neurodegeneration, presumably

via an acquired toxicity. Studies of the mutants strongly suggest that abnormally increased interactions of these mutant proteins with other proteins constitute a cause of disease (22–25). Therefore we screened for UCH-L1-interacting proteins using a coIP assay and subsequent LC-MS/MS analysis. We found that tubulin is a novel UCH-L1-interacting protein, and that the interactions of UCH-L1^{I93M} with these proteins are increased compared with those of UCH-L1^{WT} (Fig. 5B). We have also shown that UCH-L1^{I93M} promotes tubulin polymerization and stabilizes microtubules (Fig. 6B–D). UCH-L1^{I93M} and paclitaxel coordinately induced neuronal cell death (Fig. 6F). Together with the fact that tightly regulated tubulin polymerization is essential for neurons to function and remain viable, and that abnormal microtubule dynamics and tubulin polymerization are associated with several neurodegenerative diseases (37,38), our results strongly suggest that aberrant tubulin polymerization caused by mutant UCH-L1 at least partly constitutes a toxic function of mutant UCH-L1. Other than tubulin, mutant UCH-L1 interacts with multiple proteins (Figs 1F and 5A). These other interactors may also be involved in the mechanism of UCH-L1-mediated neurodegeneration (Fig. 7D). We have identified some of these interactors (T.K. and K.W., unpublished data), and these proteins are currently under investigation.

It is known that the majority of PD cases occur sporadically, and that oxidative/carbonyl stresses are elevated in PD brains (12,13). However, the molecular mechanisms underlying the causes of sporadic PD have remained largely unknown. Choi *et al.* (12) have shown that UCH-L1 is a major target of carbonyl damage associated with sporadic PD, implying that carbonyl-modified UCH-L1 is involved in the cause of these sporadic diseases. In the present study, we found that carbonyl-modified UCH-L1 and UCH-L1^{I93M} share molecular and functional properties. Importantly, both UCH-L1s display shared properties in all of the experiments we performed (Supplementary Material, Table S2). These results strongly suggest that carbonyl-modified UCH-L1 is also toxic to neurons and constitutes one of the causes of sporadic PD. Considering that UCH-L1 is abundant in the brain (5), and that UCH-L1 is a major target of carbonyl damage in PD brains (12), it is possible that carbonyl-modified UCH-L1 is the major cause of the disease.

It has been reported that UCH-L1 mRNA is expressed abundantly in dopaminergic neurons in the human brain (41). Abundant expression of UCH-L1 protein in dopaminergic neurons was also observed in mouse brains (Supplementary Material, Fig. S4 and S5). Dopaminergic neurons are particularly exposed to oxidative and carbonyl stresses because dopamine can auto-oxidize into toxic dopamine quinone, superoxide radicals and hydrogen peroxide (42). In addition, it has been reported that oxidative stresses in dopaminergic neurons in sporadic PD brains are higher than the stresses in control brains (30). Thus, in PD, UCH-L1^{I93M} or oxidative/carbonyl-modified UCH-L1 is possibly overproduced in dopaminergic neurons, leading to the selective loss of dopaminergic neurons (Fig. 7D).

Oxidatively modified UCH-L1 has also been found in the brains of both familial and sporadic Alzheimer's disease (AD) patients (12,43,44). AD is characterized pathologically by deposition of the amyloid β-protein in the form of amyloid plaques in the brain, and the deposition of the amyloid β is thought to be a major cause of both familial and sporadic AD (20). Thus, although it is possible that toxicity of carbonyl-modified UCH-L1 is involved in amyloid β-mediated neurodegeneration in AD, carbonyl-modified UCH-L1 may not be the primary cause of AD. A recent report has shown that brains from patients with sporadic PD and AD contain decreased levels of UCH-L1 (30 and 50% decrease, respectively) (12). Gong *et al.* (45) showed that the introduction of exogenous UCH-L1 rescued the synaptic and cognitive functions of AD model mice, which exhibit decreased levels of UCH-L1 in their hippocampi. We have also shown that mice deficient in UCH-L1 exhibit memory dysfunction (46). These findings indicate that a reduction in the levels of functional UCH-L1 may contribute to the pathogenesis of AD. Oxidative modification of several proteins, including antioxidant proteins, is found in mice deficient in UCH-L1 (47), suggesting involvement of these proteins in AD. Since diminution of the proteasome activity may lead to neurodegeneration (48), it is also possible that decreased UCH-L1 function leads to dysfunction of the ubiquitin-proteasome system and this dysfunction contributes to neurodegeneration in AD. On the contrary, mice deficient in UCH-L1 do not exhibit progressive dopaminergic cell loss, indicating that a loss or decrease in the level of UCH-L1 is not the main cause of PD. Investigation of the relationship between the specificity of brain areas that is affected by oxidative stress and genetic or environmental factors should generate further insights into the mechanism of oxidative stress in the pathogenesis of sporadic PD and AD.

In conclusion, familial PD-associated UCH-L1^{I93M} and carbonyl-modified UCH-L1, which is associated with sporadic PD, display common aberrant properties. Thus, UCH-L1^{I93M} is a useful tool for studying the molecular mechanism underlying sporadic PD. We propose that the abnormal interactions of UCH-L1 variants with other proteins including tubulin constitute one of the causes of not only familial PD associated with UCH-L1^{I93M}, but also sporadic PD, and can be therapeutic targets for these diseases and possibly for other neurodegenerative diseases.

MATERIALS AND METHODS

Plasmids

pCI-neo-hUCH-L1 plasmids containing human WT UCH-L1 and UCH-L1 variants with or without FLAG tag were prepared as described previously (49) or generated using a QuikChange Site-Directed Mutagenesis Kit (Stratagene, La Jolla, CA, USA). The expression plasmid pCR3-hα-synuclein containing FLAG-tagged human α-synuclein was kindly donated by Ryosuke Takahashi (Kyoto University, Kyoto, Japan) and Yuzuru Imai (Tohoku University, Miyagi, Japan) (50). The pcDNA3-hSOD1 expression plasmids containing WT, A4V, G85R or G93A mutant SOD1, and pCI-hα-synuclein expression plasmids containing WT, A30P or A53T mutant α-synuclein were prepared as described previously (17). The expression plasmid pEF-hUCH-L1 containing WT UCH-L1 was constructed by ligating the cDNA

encoding UCH-L1 into pEF-BOS vector (51). The bacterial expression plasmid pPROTetE-hUCH-L1 containing 6HN-tagged UCH-L1 was prepared as described previously. pGEX-hUCH-L1 bacterial expression plasmids containing WT, I93M or R63A UCH-L1 with a GST-tag were constructed by ligating the cDNA encoding each UCH-L1 into pGEX-6P-1 vector (GE Healthcare UK Ltd, Buckinghamshire HP7 9NA, UK).

Cell culture and transfection

Neuro2a, SH-SY5Y, COS-7 and HeLa cells were maintained in Dulbecco's modified Eagle's medium (Sigma, St Louis, MO, USA) supplemented with 10% fetal bovine serum (JRH Biosciences, Lenexa, KS, USA). NIH-3T3 cells stably expressing human UCH-L1 with a FLAG-HA double-tag at the N terminus were cultured as described previously (49). Transient transfection of Neuro2a, SH-SY5Y and COS-7 cells with each vector was performed using the FuGENE 6 Transfection Reagent (Roche Diagnostics, Indianapolis, IN, USA), Trans-Fectin Lipid Reagent (Bio-Rad, Hercules, CA, USA) and Lipofectamine Reagent (Invitrogen, Carlsbad, CA, USA), respectively. For the experiments investigating the carbonyl modification of UCH-L1, cells were incubated at 37°C for 90 min with each carbonyl compound or H_2O_2 in PBS containing 5 mM glucose, 0.3 mM $CaCl_2$ and 0.62 mM $MgCl_2$.

Immunoblotting

SDS–PAGE was performed under reducing conditions. Immunoblotting was performed according to standard procedures. The preparation of detergent (1% Triton X-100)-soluble and -insoluble fractions was performed as described previously (17). Mouse anti-α-tubulin and anti-β-tubulin antibodies were purchased from Sigma. Rabbit anti-α-tubulin and anti-β-tubulin antibodies were from Cell Signaling (Danvers, MA, USA). Mouse anti-HNE and rabbit anti-HNE antibodies were from Oxis (Portland, OR, USA) and Alpha Diagnostic (San Antonio, TX, USA), respectively. Antibodies against SOD1, UCH-L1 and reduced-HNE were purchased from Stressgen Bioreagents (Victoria, BC, Canada), UltraClone (England, UK) and Calbiochem (Darmstadt, Germany), respectively. Anti-β-actin, ubiquitin and FLAG antibodies were from Sigma. The antibody against α-synuclein was from Chemicon (Temecula, CA, USA). For immunoblotting with anti-reduced HNE antibody, the proteins on a PVDF membrane were reduced with 10 mM $NaBH_4$ in Tris-buffered saline for 30 min at room temperature before being reacted with anti-reduced HNE antibody. Carbonyl modification of proteins was detected using an OxyBlot Protein Oxidation Detection Kit (Chemicon) containing an anti-DNP antibody.

Immunoprecipitation

Immunoprecipitation was performed as previously described (52). Cells were harvested by cold immunoprecipitation buffer (15 mM Tris pH 7.5, 120 mM NaCl, 25 mM KCl, 2 mM EGTA, 2 mM EDTA, 0.5% Triton X-100 and protease inhibitors). The lysates were centrifuged at 20 000*g* for 10 min at 4°C. The supernatant was subjected to immunoprecipitation. Lysates (1 mg protein in immunoprecipitation buffer) were incubated with 5 μg of antibody for 12 h. Twenty microliters of protein G Sepharose (GE Healthcare) was then added, and incubation was continued for 1 h. For the immunoprecipitation of FLAG-tagged proteins, lysates (1–2 mg protein in immunoprecipitation buffer) were incubated with 30 μl anti-FLAG M2 affinity gel (Sigma) for 2 h. After the beads were washed three times with immunoprecipitation buffer, proteins were eluted with SDS sample buffer (10 mM Tris, pH 7.8, 3% SDS, 5% glycerol and 0.02% bromophenol blue). In some experiments, proteins were eluted with SDS sample buffer containing 2% 2-mercaptoethanol. For the immunoprecipitation of endogenous UCH-L1 (Fig. 5D), 100 μg anti-UCH-L1 antibody (53) or 100 μg normal rabbit IgG (Santa Cruz Biotechnology, Santa Cruz, CA, USA) was immobilized to 100 μl of protein G beads using a Seize X Protein G Immnoprecipitation Kit (Pierce, Rockford, IL, USA). Cell lysates (1 mg protein in 50 mM Tris, pH 7.5, 150 mM NaCl, 5 mM EDTA, 0.25% Triton X-100 and protease inhibitors) were incubated with 25 μl of beads for 12 h. Protein G beads without antibody and protein G beads cross-linked with normal rabbit IgG were used as controls.

Mass spectrometry analysis

Protein bands were sliced from the gel and subjected to in-gel trypsin digestion, and LC-MS/MS analysis was performed at APRO Life Science Institute, Inc. (Naruto, Japan) as a custom service.

Circular dichroism

CD measurements of 0.1 mg/ml (4 μM) of recombinant human UCH-L1 without a tag (Boston Biochem, Cambridge, MA, USA) in 20 mM sodium phosphate buffer (pH 8.0) were performed as described previously (9,10). Since two cysteine residues in UCH-L1, Cys-90 and Cys-152, are major targets of HNE modification (Fig. 4), 4 μM UCH-L1 was reacted with 8 μM HNE. Far UV CD spectra (190–250 nm) were recorded in a 1 mm quartz cuvette on a Jasco J-820 spectropolarimeter (Jasco, Tokyo, Japan) equipped with a temperature controller by scanning at a rate of 50 nm/min at 25°C. For all spectra, 12 scans were averaged. All CD spectra were corrected by background subtraction of the spectrum obtained with buffer alone and smoothed. Spectra were analyzed for the percentage of secondary structural elements by a computer program, based on an algorithm that compares experimental spectra with those of known proteins (54).

Preparation of recombinant proteins

6HN-tagged human UCH-L1 proteins were prepared as described previously (9). For purification of UCH-L1 without a tag, the pGEX UCH-L1 vectors were transformed into *Escherichia coli* BL21. Production of fusion proteins was induced by the addition of isopropyl-β-D-thiogalactopyranoside to a final concentration of 0.5 mM. After a 4 h induction at 37°C, the cells were harvested and lysed by sonication in PBS containing 1% Triton X-100 and protease inhibitors. Puri-

fication of GST-tagged UCH-L1 was performed using glutathione Sepharose 4B (GE Healthcare), and UCH-L1 was released from GST by digestion using PreScission Protease (GE Healthcare). Purified proteins were resolved by SDS–PAGE under reducing conditions and visualized by Coomassie brilliant blue R-250 to confirm purity (Supplementary Material, Fig. S6).

Pull-down assay

TALON resin (Clontech, Palo Alto, CA, USA) was blocked with 3% BSA for 1 h in order to prevent non-specific binding of tubulin (data not shown) and washed three times with PBS containing 0.05% Triton X-100. Five micrograms of recombinant UCH-L1 with an HN tag and 5 μg of purified tubulin (>99% pure tubulin, Cytoskeleton, Denver, CO, USA) were mixed and incubated for 4 h in PBS containing 0.05% Triton X-100. As a control, vehicle was mixed instead of UCH-L1. Twenty microliters of TALON resin blocked with BSA was then added, and incubation was continued for 1 h. After beads were washed three times with PBS containing 0.05% Triton X-100, proteins were eluted with SDS sample buffer.

Tubulin polymerization assay

An *in vitro* tubulin polymerization assay was performed using a tubulin polymerization assay kit, OD based, >99% pure tubulin (Cytoskeleton), according to the manufacturer's protocol. Briefly, recombinant UCH-L1 without a tag and tubulin were mixed to give a final concentration of 0.05 mg/ml UCH-L1 and 3 mg/ml tubulin in tubulin polymerization buffer (80 mM PIPES, pH 6.9, 2 mM $MgCl_2$, 0.5 mM EGTA, 1 mM GTP, 5% glycerol) and subjected to a tubulin polymerization assay. As a control, vehicle was mixed instead of UCH-L1. Since two cysteine residues in UCH-L1 are major targets of HNE modification (Fig. 4), 40 μM UCH-L1 was reacted with 80 μM HNE to prepare the HNE-modified UCH-L1. To analyze the interaction between UCH-L1 and polymerized tubulin, the polymerized tubulin was pelleted by centrifugation after a tubulin polymerization assay. The supernatant (100 μl) was mixed with 50 μl of 3× SDS sample buffer (30 mM Tris, pH 7.8, 9% SDS, 15% glycerol, 0.06% bromophenol blue). The pellet was washed twice with tubulin polymerization buffer and then dissolved in 150 μl of SDS sample buffer.

Preparation of cell extracts containing soluble and polymeric tubulin

Preparation of soluble and polymeric fractions of tubulin was performed as described (55) with slight modification. Briefly, cells were washed very gently with a microtubule stabilizing buffer (0.1 M *N*-morpholinoethanesulfonic acid, pH 6.75, 1 mM $MgSO_4$, 2 mM EGTA, 0.1 mM EDTA, 4 M glycerol). Soluble proteins were extracted at 37°C for 5 min in microtubule stabilizing buffer containing 0.04% saponin. The remaining cytoskeletal fraction in the culture dish was washed with microtubule stabilizing buffer containing 0.4% saponin and dissolved in SDS sample buffer.

Quantitative assessment of cell death

Neuro2a cells were transfected with plasmids. Four hours after transfection, neuronal cell differentiation was induced by addition of 5 mM dibutyryl cAMP as described in the literature (40), and cells were incubated for 24 h. Cells were then incubated with or without 5 μM paclitaxel for another 24 h. Cell death was assessed by a lactate dehydrogenase release assay, as described previously (17).

Statistical analysis

For comparison of two groups, the statistical difference was determined by Student's *t*-test.

SUPPLEMENTARY MATERIAL

Supplementary Material is available at HMG Online.

ACKNOWLEDGEMENTS

We thank Dr Ryosuke Takahashi (Kyoto University) and Dr Yuzuru Imai (Tohoku University) for the gift of pCR3-hα-synuclein plasmid, Dr Yasuyuki Suzuki (National Institute of Neuroscience) for valuable discussion; Naoki Takagaki (National Institute of Neuroscience) for support with English.

Conflict of Interest statement. None declared.

FUNDING

This work was supported by Grants-in-Aid for Scientific Research of Japan Society for the Promotion of Science; Research Grant in Priority Area Research of the Ministry of Education, Culture, Sports, Science and Technology, Japan; Grants-in-Aid for Scientific Research of the Ministry of Health, Labour and Welfare, Japan; Program for Promotion of Fundamental Studies in Health Sciences of the National Institute of Biomedical Innovation (NIBIO), Japan; New Energy and Industrial Technology Development Organization (NEDO), Japan.

REFERENCES

1. Leroy, E., Boyer, R., Auburger, G., Leube, B., Ulm, G., Mezey, E., Harta, G., Brownstein, M.J., Jonnalagada, S., Chernova, T. *et al.* (1998) The ubiquitin pathway in Parkinson's disease. *Nature*, **395**, 451–452.
2. Setsuie, R., Wang, Y.L., Mochizuki, H., Osaka, H., Hayakawa, H., Ichihara, N., Li, H., Furuta, A., Sano, Y., Sun, Y.J. *et al.* (2007) Dopaminergic neuronal loss in transgenic mice expressing the Parkinson's disease-associated UCH-L1 I93M mutant. *Neurochem. Int.*, **50**, 119–129.
3. Maraganore, D.M., Lesnick, T.G., Elbaz, A., Chartier-Harlin, M.C., Gasser, T., Kruger, R., Hattori, N., Mellick, G.D., Quattrone, A., Satoh, J. *et al.* (2004) UCHL1 is a Parkinson's disease susceptibility gene. *Ann. Neurol.*, **55**, 512–521.
4. Healy, D.G., Abou-Sleiman, P.M., Casas, J.P., Ahmadi, K.R., Lynch, T., Gandhi, S., Muqit, M.M., Foltynie, T., Barker, R., Bhatia, K.P. *et al.* (2006) UCHL-1 is not a Parkinson's disease susceptibility gene. *Ann. Neurol.*, **59**, 627–633.
5. Wilkinson, K.D., Lee, K.M., Deshpande, S., Duerksen-Hughes, P., Boss, J.M. and Pohl, J. (1989) The neuron-specific protein PGP 9.5 is a ubiquitin carboxyl-terminal hydrolase. *Science*, **246**, 670–673.

6. Larsen, C.N., Krantz, B.A. and Wilkinson, K.D. (1998) Substrate specificity of deubiquitinating enzymes: ubiquitin C-terminal hydrolases. *Biochemistry*, **37**, 3358–3368.
7. Liu, Y., Fallon, L., Lashuel, H.A., Liu, Z. and Lansbury, P.T., Jr (2002) The UCH-L1 gene encodes two opposing enzymatic activities that affect alpha-synuclein degradation and Parkinson's disease susceptibility. *Cell*, **111**, 209–218.
8. Osaka, H., Wang, Y.L., Takada, K., Takizawa, S., Setsuie, R., Li, H., Sato, Y., Nishikawa, K., Sun, Y.J., Sakurai, M. *et al.* (2003) Ubiquitin carboxy-terminal hydrolase L1 binds to and stabilizes monoubiquitin in neuron. *Hum. Mol. Genet.*, **12**, 1945–1958.
9. Nishikawa, K., Li, H., Kawamura, R., Osaka, H., Wang, Y.L., Hara, Y., Hirokawa, T., Manago, Y., Amano, T., Noda, M. *et al.* (2003) Alterations of structure and hydrolase activity of parkinsonism-associated human ubiquitin carboxyl-terminal hydrolase L1 variants. *Biochem. Biophys. Res. Commun.*, **304**, 176–183.
10. Naito, S., Mochizuki, H., Yasuda, T., Mizuno, Y., Furusaka, M., Ikeda, S., Adachi, T., Shimizu, H.M., Suzuki, J., Fujiwara, S. *et al.* (2006) Characterization of multimetric variants of ubiquitin carboxyl-terminal hydrolase L1 in water by small-angle neutron scattering. *Biochem. Biophys. Res. Commun.*, **339**, 717–725.
11. Saigoh, K., Wang, Y.L., Suh, J.G., Yamanishi, T., Sakai, Y., Kiyosawa, H., Harada, T., Ichihara, N., Wakana, S., Kikuchi, T. *et al.* (1999) Intragenic deletion in the gene encoding ubiquitin carboxy-terminal hydrolase in gad mice. *Nat. Genet.*, **23**, 47–51.
12. Choi, J., Levey, A.I., Weintraub, S.T., Rees, H.D., Gearing, M., Chin, L.S. and Li, L. (2004) Oxidative modifications and down-regulation of ubiquitin carboxyl-terminal hydrolase L1 associated with idiopathic Parkinson's and Alzheimer's diseases. *J. Biol. Chem.*, **279**, 13256–13264.
13. Ischiropoulos, H. and Beckman, J.S. (2003) Oxidative stress and nitration in neurodegeneration: cause, effect, or association? *J. Clin. Invest.*, **111**, 163–169.
14. Lowe, J., McDermott, H., Landon, M., Mayer, R.J. and Wilkinson, K.D. (1990) Ubiquitin carboxyl-terminal hydrolase (PGP 9.5) is selectively present in ubiquitinated inclusion bodies characteristic of human neurodegenerative diseases. *J. Pathol.*, **161**, 153–160.
15. Lee, M.K., Stirling, W., Xu, Y., Xu, X., Qui, D., Mandir, A.S., Dawson, T.M., Copeland, N.G., Jenkins, N.A. and Price, D.L. (2002) Human alpha-synuclein-harboring familial Parkinson's disease-linked Ala-53→Thr mutation causes neurodegenerative disease with alpha-synuclein aggregation in transgenic mice. *Proc. Natl Acad. Sci. USA*, **99**, 8968–8973.
16. Johnston, J.A., Dalton, M.J., Gurney, M.E. and Kopito, R.R. (2000) Formation of high molecular weight complexes of mutant Cu,Zn-superoxide dismutase in a mouse model for familial amyotrophic lateral sclerosis. *Proc. Natl Acad. Sci. USA*, **97**, 12571–12576.
17. Kabuta, T., Suzuki, Y. and Wada, K. (2006) Degradation of amyotrophic lateral sclerosis-linked mutant Cu,Zn-superoxide dismutase proteins by macroautophagy and the proteasome. *J. Biol. Chem.*, **281**, 30524–30533.
18. Lewis, J., McGowan, E., Rockwood, J., Melrose, H., Nacharaju, P., Van Slegtenhorst, M., Gwinn-Hardy, K., Paul Murphy, M., Baker, M., Yu, X. *et al.* (2000) Neurofibrillary tangles, amyotrophy and progressive motor disturbance in mice expressing mutant (P301L) tau protein. *Nat. Genet.*, **25**, 402–405.
19. Ardley, H.C., Scott, G.B., Rose, S.A., Tan, N.G. and Robinson, P.A. (2004) UCH-L1 aggresome formation in response to proteasome impairment indicates a role in inclusion formation in Parkinson's disease. *J. Neurochem.*, **90**, 379–391.
20. Haass, C. and Selkoe, D.J. (2007) Soluble protein oligomers in neurodegeneration: lessons from the Alzheimer's amyloid beta-peptide. *Nat. Rev. Mol. Cell Biol.*, **8**, 101–112.
21. Arrasate, M., Mitra, S., Schweitzer, E.S., Segal, M.R. and Finkbeiner, S. (2004) Inclusion body formation reduces levels of mutant huntingtin and the risk of neuronal death. *Nature*, **431**, 805–810.
22. Pasinelli, P., Belford, M.E., Lennon, N., Bacskai, B.J., Hyman, B.T., Trotti, D. and Brown, R.H., Jr (2004) Amyotrophic lateral sclerosis-associated SOD1 mutant proteins bind and aggregate with Bcl-2 in spinal cord mitochondria. *Neuron*, **43**, 19–30.
23. Zhang, F., Strom, A.L., Fukada, K., Lee, S., Hayward, L.J. and Zhu, H. (2007) Interaction between familial amyotrophic lateral sclerosis (ALS)-linked SOD1 mutants and the dynein complex. *J. Biol. Chem.*, **282**, 16691–16699.
24. Urushitani, M., Sik, A., Sakurai, T., Nukina, N., Takahashi, R. and Julien, J.P. (2006) Chromogranin-mediated secretion of mutant superoxide dismutase proteins linked to amyotrophic lateral sclerosis. *Nat. Neurosci.*, **9**, 108–118.
25. Cuervo, A.M., Stefanis, L., Fredenburg, R., Lansbury, P.T. and Sulzer, D. (2004) Impaired degradation of mutant alpha-synuclein by chaperone-mediated autophagy. *Science*, **305**, 1292–1295.
26. Schaffar, G., Breuer, P., Boteva, R., Behrends, C., Tzvetkov, N., Strippel, N., Sakahira, H., Siegers, K., Hayer-Hartl, M. and Hartl, F.U. (2004) Cellular toxicity of polyglutamine expansion proteins: mechanism of transcription factor deactivation. *Mol. Cell*, **15**, 95–105.
27. Uchida, K. (2000) Role of reactive aldehyde in cardiovascular diseases. *Free Radic. Biol. Med.*, **28**, 1685–1696.
28. Uchida, K. (2003) Histidine and lysine as targets of oxidative modification. *Amino Acids*, **25**, 249–257.
29. Stadtman, E.R. (1993) Oxidation of free amino acids and amino acid residues in proteins by radiolysis and by metal-catalyzed reactions. *Annu. Rev. Biochem.*, **62**, 797–821.
30. Yoritaka, A., Hattori, N., Uchida, K., Tanaka, M., Stadtman, E.R. and Mizuno, Y. (1996) Immunohistochemical detection of 4-hydroxynonenal protein adducts in Parkinson disease. *Proc. Natl Acad. Sci. USA*, **93**, 2696–2701.
31. Castellani, R.J., Perry, G., Siedlak, S.L., Nunomura, A., Shimohama, S., Zhang, J., Montine, T., Sayre, L.M. and Smith, M.A. (2002) Hydroxynonenal adducts indicate a role for lipid peroxidation in neocortical and brainstem Lewy bodies in humans. *Neurosci. Lett.*, **319**, 25–28.
32. Das, C., Hoang, Q.Q., Kreinbring, C.A., Luchansky, S.J., Meray, R.K., Ray, S.S., Lansbury, P.T., Ringe, D. and Petsko, G.A. (2006) Structural basis for conformational plasticity of the Parkinson's disease-associated ubiquitin hydrolase UCH-L1. *Proc. Natl Acad. Sci. USA*, **103**, 4675–4680.
33. Tiwari, A., Xu, Z. and Hayward, L.J. (2005) Aberrantly increased hydrophobicity shared by mutants of Cu,Zn-superoxide dismutase in familial amyotrophic lateral sclerosis. *J. Biol. Chem.*, **280**, 29771–29779.
34. Richardson, J.S. and Richardson, D.C. (2002) Natural beta-sheet proteins use negative design to avoid edge-to-edge aggregation. *Proc. Natl Acad. Sci. USA*, **99**, 2754–2759.
35. Lee, J.J. and Swain, S.M. (2006) Peripheral neuropathy induced by microtubule-stabilizing agents. *J. Clin. Oncol.*, **24**, 1633–1642.
36. Figueroa-Masot, X.A., Hetman, M., Higgins, M.J., Kokot, N. and Xia, Z. (2001) Taxol induces apoptosis in cortical neurons by a mechanism independent of Bcl-2 phosphorylation. *J. Neurosci.*, **21**, 4657–4667.
37. Panda, D., Samuel, J.C., Massie, M., Feinstein, S.C. and Wilson, L. (2003) Differential regulation of microtubule dynamics by three- and four-repeat tau: implications for the onset of neurodegenerative disease. *Proc. Natl Acad. Sci. USA*, **100**, 9548–9553.
38. Fanara, P., Banerjee, J., Hueck, R.V., Harper, M.R., Awada, M., Turner, H., Husted, K.H., Brandt, R. and Hellerstein, M.K. (2007) Stabilization of hyperdynamic microtubules is neuroprotective in amyotrophic lateral sclerosis. *J. Biol. Chem.*, **282**, 23465–23472.
39. Tam, S., Geller, R., Spiess, C. and Frydman, J. (2006) The chaperonin TRiC controls polyglutamine aggregation and toxicity through subunit-specific interactions. *Nat. Cell Biol.*, **8**, 1155–1162.
40. Kitamura, A., Kubota, H., Pack, C.G., Matsumoto, G., Hirayama, S., Takahashi, Y., Kimura, H., Kinjo, M., Morimoto, R.I. and Nagata, K. (2006) Cytosolic chaperonin prevents polyglutamine toxicity with altering the aggregation state. *Nat. Cell Biol.*, **8**, 1163–1170.
41. Solano, S.M., Miller, D.W., Augood, S.J., Young, A.B. and Penney, J.B., Jr (2000) Expression of alpha-synuclein, parkin, and ubiquitin carboxy-terminal hydrolase L1 mRNA in human brain: genes associated with familial Parkinson's disease. *Ann. Neurol.*, **47**, 201–210.
42. Lotharius, J. and Brundin, P. (2002) Pathogenesis of Parkinson's disease: dopamine, vesicles and alpha-synuclein. *Nat. Rev. Neurosci.*, **3**, 932–942.
43. Castegna, A., Aksenov, M., Aksenova, M., Thongboonkerd, V., Klein, J.B., Pierce, W.M., Booze, R., Markesbery, W.R. and Butterfield, D.A. (2002) Proteomic identification of oxidatively modified proteins in Alzheimer's disease brain. Part I: creatine kinase BB, glutamine synthase, and ubiquitin carboxy-terminal hydrolase L-1. *Free Radic. Biol. Med.*, **33**, 562–571.
44. Butterfield, D.A., Gnjec, A., Poon, H.F., Castegna, A., Pierce, W.M., Klein, J.B. and Martins, R.N. (2006) Redox proteomics identification of

oxidatively modified brain proteins in inherited Alzheimer's disease: an initial assessment. *J. Alzheimers Dis.*, **10**, 391–397.
45. Gong, B., Cao, Z., Zheng, P., Vitolo, O.V., Liu, S., Staniszewski, A., Moolman, D., Zhang, H., Shelanski, M. and Arancio, O. (2006) Ubiquitin hydrolase Uch-L1 rescues beta-amyloid-induced decreases in synaptic function and contextual memory. *Cell*, **126**, 775–788.
46. Sakurai, M., Sekiguchi, M., Zushida, K., Yamada, K., Nagamine, S., Kabuta, T. and Wada, K. (2008) Reduction of memory in passive avoidance learning, exploratory behavior and synaptic plasticity in mice with a spontaneous deletion in the ubiquitin C-terminal hydrolase L1 gene. *Eur. J. Neurosci.*, in press.
47. Castegna, A., Thongboonkerd, V., Klein, J., Lynn, B.C., Wang, Y.L., Osaka, H., Wada, K. and Butterfield, D.A. (2004) Proteomic analysis of brain proteins in the gracile axonal dystrophy (gad) mouse, a syndrome that emanates from dysfunctional ubiquitin carboxyl-terminal hydrolase L-1, reveals oxidation of key proteins. *J. Neurochem.*, **88**, 1540–1546.
48. Halliwell, B. (2006) Proteasomal dysfunction: a common feature of neurodegenerative diseases? Implications for the environmental origins of neurodegeneration. *Antioxid. Redox Signal.*, **8**, 2007–2019.
49. Sakurai, M., Ayukawa, K., Setsuie, R., Nishikawa, K., Hara, Y., Ohashi, H., Nishimoto, M., Abe, T., Kudo, Y., Sekiguchi, M. *et al.* (2006) Ubiquitin C-terminal hydrolase L1 regulates the morphology of neural progenitor cells and modulates their differentiation. *J. Cell Sci.*, **119**, 162–171.
50. Imai, Y., Soda, M. and Takahashi, R. (2000) Parkin suppresses unfolded protein stress-induced cell death through its E3 ubiquitin-protein ligase activity. *J. Biol. Chem.*, **275**, 35661–35664.
51. Mizushima, S. and Nagata, S. (1990) pEF-BOS, a powerful mammalian expression vector. *Nucleic Acids Res.*, **18**, 5322.
52. Kabuta, T., Hakuno, F., Asano, T. and Takahashi, S. (2002) Insulin receptor substrate-3 functions as transcriptional activator in the nucleus. *J. Biol. Chem.*, **277**, 6846–6851.
53. Sano, Y., Furuta, A., Setsuie, R., Kikuchi, H., Wang, Y.L., Sakurai, M., Kwon, J., Noda, M. and Wada, K. (2006) Photoreceptor cell apoptosis in the retinal degeneration of Uchl3-deficient mice. *Am. J. Pathol.*, **169**, 132–141.
54. Yang, J.T., Wu, C.S. and Martinez, H.M. (1986) Calculation of protein conformation from circular dichroism. *Methods Enzymol.*, **130**, 208–269.
55. Joshi, H.C. and Cleveland, D.W. (1989) Differential utilization of beta-tubulin isotypes in differentiating neurites. *J. Cell Biol.*, **109**, 663–673.